



Published in final edited form as:

ACS Infect Dis. 2017 August 11; 3(8): 575–584. doi:10.1021/acsinfecdis.7b00052.

Optimized fluorescence complementation platform for visualizing *Salmonella* effector proteins reveals distinctly different intracellular niches in different cell types

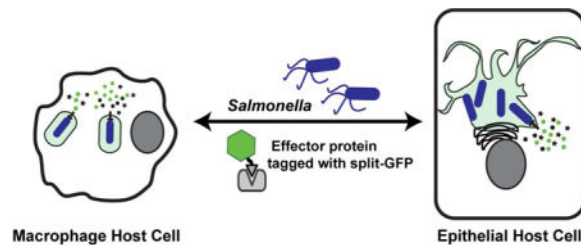
Alexandra M. Young, Michael Minson, Sarah E. McQuate, and Amy E. Palmer*

Department of Chemistry and Biochemistry, BioFrontiers Institute, UCB 596, 3415 Colorado Ave, University of Colorado, Boulder, CO 80303

Abstract

The bacterial pathogen *Salmonella* uses sophisticated type III secretion systems (T3SS) to translocate and deliver bacterial effector proteins into host cells to establish infection. Monitoring these important virulence determinants in the context of live infections is a key step in defining the dynamic interface between the host and pathogen. Here, we provide a modular labeling platform based on fluorescence complementation with split-GFP that permits facile tagging of new *Salmonella* effector proteins. We demonstrate enhancement of split-GFP complementation signals by manipulating the promoter or by multimerizing the fluorescent tag and visualize three effector proteins, SseF, SseG and SlrP, that have never before been visualized over time during infection of live cells. Using this platform, we developed a methodology for visualizing effector proteins in primary macrophage cells for the first time and reveal distinct differences in effector defined intracellular niche between primary macrophage and commonly used HeLa and RAW cell lines.

Table of Contents Use Only



*To whom correspondence should be addressed: amy.palmer@colorado.edu, 303-492-1945.

SUPPORTING INFORMATION

All experimental methods as well as figures illustrating the cloning layout, fluorescence intensity profiles, growth curves, time course imaging, filament phenotypes, bacterial phenotypes and reporter conditions are included in Supporting Information.

AUTHOR CONTRIBUTIONS

A.M.Y, M.M., S.E.M., and A.E.P. planned experiments and analyzed data. A.M.Y., M.M. and S.E.M. collected data. A.M.Y., M.M., and A.E.P. wrote the paper.

CONFLICT OF INTEREST STATEMENT

The authors declare no competing financial interest.

Keywords

Host-pathogen interface; Bacterial effector proteins; Live cell imaging; Split-GFP; *Salmonella*

Visualizing the host-pathogen interface between infected mammalian cells and *Salmonella* is a key step in unraveling the complex dynamics of infection biology. *Salmonella enterica* serovar Typhimurium (hereafter referred to as *Salmonella*) infects a range of animal hosts, including humans, and is a major cause of enteric illness. *Salmonella* is equipped with complex nanomachines, called Type III Secretion Systems (T3SSs) that span both bacterial membranes and penetrate the membrane of a host cell to inject bacterial proteins, also called effector proteins, directly into the host cytosol¹. The cocktail of translocated bacterial effector proteins enables *Salmonella* to manipulate signaling cascades to influence host cellular processes to promote infection (reviewed in^{2,3}). *Salmonella* has two distinct T3SSs. T3SS-1 is expressed upon contact with epithelial host cells and T3SS-1 translocated effector proteins promote bacterial internalization and encapsulation in a phagosome-like compartment called the *Salmonella* containing vacuole (SCV)⁴. T3SS-2 is expressed upon bacterial internalization and its associated effector proteins are important for maturation of the SCV, cultivating a replicative niche, and interfering with host cell immune responses^{5,6}. The coordinated activity of effector proteins is crucial to bacterial survival, replication and dissemination within a host organism. However, the distinct functions of many effector proteins remain poorly understood. Defining the localization of effector proteins within the host cell at different stages of infection is important for elucidating how the pathogen manipulates host cell biology, and spatiotemporal information about an effector protein's localization in the context of infection can highlight that protein's role in the infection process. Given that *Salmonella* infects both epithelial cells and macrophages, we set out to establish tools for visualizing *Salmonella* effector proteins over the course of infection in both model systems to define whether effector proteins establish distinct niches in different environments.

In establishing a robust and versatile platform, we felt that important features included: compatibility with live cell imaging, single cell resolution, ability to tag translocated effector proteins in the context of infection and in the presence of the cohort of other effector proteins, and functionality in both intracellular niches for *Salmonella* (epithelial cells and primary macrophages). The importance of live cell imaging for defining the interface between pathogen and host derives from the observation that isolated snap shots often fail to capture complex dynamic phenotypes such as dispersion and coalescence of the SCV⁷, and that cell fixation can alter infection phenotypes, such as the integrity of membrane tubules that emanate from the SCV^{1,8}. The need for single cell resolution was motivated by widely observed heterogeneity in infection phenotypes from cell to cell. For example, *Salmonella* can use different mechanisms to invade individual epithelial cells^{2,3,8-10}, can replicate inside the SCV or escape and hyper-replicate in the cytosol of epithelial cells^{4,11}, and experience different fates in macrophages^{5-7,12}. Collectively, these cell-to-cell variations in infection phenotypes are likely due, at least in part, to the differential presence and function of effector proteins^{3,7}, demonstrating the need for techniques that capture effector protein localization and infection phenotypes, while preserving single cell heterogeneity. Finally,

transient transfection of tagged effector proteins often gives rise to different localization compared to translocated effector proteins^{13,14}, and effector proteins work cooperatively to define the host-pathogen interface², underscoring the importance of visualizing translocated effector proteins in the presence of the entire effector cohort.

While live cell imaging is important for capturing the dynamics and evolution of infection phenotypes, monitoring bacterial effector proteins is technically challenging because effector proteins must be translocated through the narrow needle-like T3SS¹⁵. The high thermodynamic stability of fluorescent proteins (FPs) interferes with translocation¹⁶, necessitating alternative approaches for effector tagging. A number of approaches have been developed to monitor effector proteins during infection, including translocation of effector proteins from bacteria to host cells^{17,18}, delivery of bacterial effector proteins to the host cytosol^{19,20}, and visualization of effector protein localization within the host cell^{14,21}. Of these tools, there are currently only two approaches capable of monitoring the fate of translocated effector proteins in living host cells during infection: a light-oxygen-voltage-sensing (LOV) domain reporter system that binds cellular flavin mononucleotides to produce a fluorescent label²¹ and a split-GFP system¹⁴. However, both approaches have limitations that have prevented widespread adoption for effector tracking long-term in host cells. The LOV-domain reporter system is small (10 kDa) and intrinsically fluorescent, but it displays weak fluorescence compared to GFP and has only been applied to highly expressed effector proteins and imaged for short periods of time²¹. Split-GFP is larger (27 kDa) and requires 2 hours for full fluorescence complementation, but it's brighter and therefore more promising for long-term (multi-hour) visualization of low expressing effector proteins during infection. However, the complexity of distinguishing the multiple variables that influence fluorescence visualization has made it difficult to apply this system to diverse effector proteins.

In this study, we optimized split-GFP tagging by developing a platform that permits facile tagging and evaluation of complementation signal intensities of different effector proteins using a suite of expression approaches. This platform enables amplification of split-GFP complementation signals by driving their expression with the promoter of the highly expressed effector protein SteA, or multimerizing the GFP11 tag. Using this platform, we tracked multiple effector proteins during live infections over 10 hours for the first time, and developed methodology for tagging and tracking of effector proteins in primary bone marrow derived macrophages (BMDMs) from immunocompetent mice, revealing distinct differences in the intracellular niche molded by effector proteins compared to commonly used cell lines. Finally, these new studies provide insight into the localization and hence function of several *Salmonella* effector proteins.

RESULTS AND DISCUSSION

Modular Split-GFP labeling platform

To facilitate visualization of *Salmonella* effector proteins during infection of live cells a modular expression platform was generated. The plasmid-based platform features an exchangeable promoter, effector, and GFP11 tag as well as a constitutively expressed fluorescent protein (FP) that serves as a bacterial marker (Fig. 1A, Fig. S1). The pACYC177 plasmid was chosen as the backbone because unlike pAYCY184, pWSK29 or plasmids

derived from pBR322, it doesn't interfere with growth or pathogenicity when expressed in *Salmonella*^{22,23}. For each effector tested, a pair of plasmids was created, one that expressed the effector under control of its endogenous promoter, and another that used the *steA* promoter, which was chosen because SteA was previously shown to express at a level sufficient for visualization with split-GFP¹⁴. SteA is expressed and translocated under both SPI-1 and SPI-2 inducing conditions, suggesting that its regulatory region would be useful in visualizing T3SS-1 or T3SS-2 translocated effector proteins.

Bacterial expression and complementation assay

One of the weaknesses of the previously developed split-GFP system was the inability to rapidly screen for fluorescence complementation in different expression contexts. Thus, we encountered limitations with this original system when we were unable to detect a number of new effector proteins, including SseF, SseG and SlrP, under their endogenous promoters and could not determine whether this issue was due to low expression, poor complementation due to steric constraints, perturbation of translocation, or rapid protein turnover in the host cell. Therefore, we developed a method to test effector protein expression and split-GFP complementation within bacteria. This assay enables comparison of effector protein expression levels under the *steA* promoter versus an effector's endogenous promoter versus expression from its endogenous locus upon integration of the tag into the chromosome, to identify the best approach for visualization of effector proteins in the context of infection.

Salmonella strains expressing an effector tagged with GFP11 were co-transformed with GFP1-10 and the GFP_{comp} signal intensity was quantified in individual bacteria as a measure of effector protein expression and split-GFP complementation (Fig. 2, Fig S2). We observed complementation in bacteria for SteA, SlrP, SseF, SseG, and SopA when these effector proteins were expressed from a plasmid under control of the *steA* promoter (Fig. 2C, Table 1). SteA has been tagged previously¹⁴, while the other four effector proteins have never been tagged for visualization during live cell infection. SopA showed high split-GFP_{comp} signals that were comparable between endogenous and the *steA* promoter. SlrP, SseF, and SseG all gave significantly higher split-GFP_{comp} signals when expressed under the *steA* promoter compared to endogenous promoters, suggesting that the *steA* promoter may be stronger than their endogenous promoters. Consistent with this notion, a previous study using a firefly luciferase reporter system to compare effector protein expression levels found that SseG and SlrP express at low levels compared to a handful of other SPI-2 encoded effector proteins²⁴.

The intensity of the fluorescence signal varied based on the expression context (Fig. 2D, Table 1). As expected, for all effector proteins, split-GFP signal intensities were higher for plasmid-based expression. Fig. 2D shows the data for plasmid-based expression of SteA (pSteA-GFP_{comp}) versus chromosomal expression (SteA-1X-GFP_{comp}). The data for other effector proteins are presented in Supporting Fig. S2. The intensity of the fluorescence signal was amplified by including a 3-fold repeat of the GFP11 tag (Fig. 2D, Table 1). All effector proteins showed an increase in complementation signal intensity for the 3X-GFP11 tag compared to 1X-GFP11 (Fig. S2), for example SteA showed an increase in signal intensity that was approximately 3-fold, indicating near stoichiometric complementation.

Based on these results, efficient complementation signals for effector proteins require a strong native promoter, plasmid-based expression using a strong promoter like the *steA* promoter, or multimerizing the GFP11 tag.

The bacterial expression and complementation assay is valuable for indicating conditions that yield strong effector protein production. However, it is important to note that other factors can limit the ability to visualize effector proteins during live cell infections, including perturbation of translocation or rapid protein turnover in the host cell. Exogenous expression of effector proteins under non-native promoters could interfere with translocation as an RNA based translocation signal in the 5' untranslated region was suggested for the effector protein GtgA²⁵. Therefore, this assay is a useful preliminary screen but cannot be used to verify translocation or detection in the host cell.

Visualization of effector proteins in live host cells

Based on the bacterial expression assay, we anticipated being able to visualize SteA, SlrP, SseF, SseG, and SopA when expressed from a plasmid under control of the SteA promoter. To visualize these proteins in host cells upon infection we generated *Salmonella* strains expressing the mRuby3²⁶ FP under control of the constitutive *rpsM* promoter, and harboring an isogenic deletion of the target effector protein. These strains were complemented by plasmid-based expression of a GFP11 tagged version of the effector. All bacterial strains displayed *in vitro* growth curves similar to wild type *Salmonella* (Fig. S3). Indeed, we observed all of the predicted effector proteins except SopA upon live cell infection of HeLa cells (Table 1, Fig. 3A). Cells were imaged beginning at 4 hours post infection, however the labeled effector proteins were not observed until approximately 7 hours post infection. SseF and SseG both localized to the SCV and associated filaments in live HeLa cells from 7–28 hours post infection, in agreement with previous immunofluorescence-based studies^{27,28}. SseF and SseG containing filaments were highly dynamic and displayed an increase in effector-GFP_{comp} signal over time, suggesting these effector proteins accumulate in the host cell over time (Fig. S4). SlrP was observed from 9–28 hours post infection and appeared diffuse in the cytosol of the host cell. This result agrees with a 2009 study that identified the cytosolic host cell protein thioredoxin as an interaction partner for SlrP²⁹. Expressed under the *steA* promoter, SlrP-GFP_{comp} signal appeared to increase in the host cell cytosol over time (Fig. S4). To our knowledge, this is the first time that these three effector proteins have been visualized live, over time, in the context of infection.

SopA was the only effector that we readily visualized via the bacterial expression assay but were unable to observe in infected host cells between 4 and 28 hours post infection. The inability to detect translocated SopA could result from inefficient T3SS translocation of exogenously expressed SopA-GFP11, rapid turnover of SopA inside the host cell, or an unavailable C-terminal-GFP11 tag in the host cytosol for complementation with GFP1-10. Because GFP1-10 localizes to the cytosol of the host cell, it will be unable to complement with a GFP11 tagged effector protein that localizes within a subcellular compartment. Epitope-tagged SopA has been shown to localize to mitochondria in fixed cells³⁰, but it has not yet been determined whether translocated SopA associates with or resides within mitochondria during live infections.

As predicted from the bacterial expression assay, only SteA and SseF were detected when expressed from a plasmid with their endogenous promoters. SseF localization was consistent between endogenous and *steA* driven expression, with an increase in the detectable GFP_{comp} signal for *steA* driven expression. As predicted from the bacterial expression assay SteA was the only effector protein visualized upon chromosomal integration of the GFP11 tag. We found that multimerizing the GFP11 tag boosted the fluorescence signal in mammalian cells (Fig. 3B,C). Finally, although chromosomal expression of SlrP-3X-GFP_{comp} and SteA-1X-GFP_{comp} gave comparable split-GFP complementation efficiencies in the bacterial expression assay, we were not able to detect SlrP-3X-GFP_{comp} in infected cells. We speculate that this could result from the fact that SteA protein is concentrated on the SCV, while SlrP is diffuse in the cytosol, leading to less contrast over the background fluorescence of cells.

SseG localization is mediated by SseF

Given our ability to visualize SseG in live host cells, we set out to examine how the localization of SseG depends on SseF. SseF and SseG have been shown to physically and functionally interact to coordinate SCV position and maintenance^{27,31–33}. These proteins have been suggested to tether the SCV to the Golgi by jointly interacting with the Golgi associated protein ACBD3³³. SseF and SseG have also been shown to associate with endocytic membranes and microtubules^{13,27} and are hypothesized to redirect host exocytic traffic from the Golgi³¹ by recruiting dynein to the SCV³⁴. Transfected SseG showed a scattered distribution in a ~ 80% of cells that co-localized with the trans-Golgi network marker TGN46¹³. In a minority of cells, transfected SseG was filamentous, co-localized with microtubules, and appeared similar to translocated SseG localization during infection¹³, suggesting differential localization when SseG is expressed alone versus translocated with the rest of the effector cohort. Given these observations, we set out to determine whether the difference in localization was due to the mode of delivery (transfection versus T3SS-mediated translocation) or the absence of SseF.

To examine the localization of SseG in the absence of SseF, we generated a *Salmonella* strain containing an isogenic *sseF/sseG* deletion while expressing SseG-GFP11 under the control of the *steA* promoter on our plasmid based platform. SseG localized to the SCV and colocalized with bacteria in the presence and absence of SseF, regardless of whether the bacteria were in a dispersed or compact formation (Fig. 4A). However, in the absence of SseF there was a globular population of SseG at the host cell periphery that didn't colocalize with bacteria (Fig. 4A) in approximately 70% of cells, whereas less than 10% of cells display peripheral SseG in the presence of SseF (Fig. 4B). Thus, in the absence of SseF, T3SS translocated SseG displays a localization pattern similar to transfected SseG, suggesting that SseF is required for proper SseG localization. There was also a change in the morphology of filaments emanating from the SCV in the absence of SseF, where SseG containing filaments appeared either punctate or thinner than in WT infections (Fig. S5). Thin LAMP1-associated filaments have been observed for infections using *Salmonella* strains lacking either SseF or SseG⁸. Our results are consistent with the observation that SseF and SseG are involved in acquiring and redirecting host cell vesicular traffic to maintain the SCV and associated filaments^{27,35}.

It is important to note that incorporation of the GFP11 tag and over expression of tagged effector proteins could perturb native interactions or localization. In cases such as SseF and SseG whose localization has been characterized in fixed cells and for whom there is information about biochemical function, phenotypes can be compared to experiments with untagged and endogenously expressed effectors. For example, previous studies of the effector protein PipB2 revealed that tagging with GFP11 didn't perturb PipB2 function¹⁴. However, the localization of new effector proteins should be interpreted with caution and probed for any perturbing effects of over expression or the presence of a tag using alternate techniques.

SlrP is localized to the cytosol in infected host cells

One advantage of the split-GFP system is the ability to target GFP1-10 to subcellular compartments in the host cell to address questions about the specific localization of effector proteins; for example, distinguishing whether an effector protein resides inside an organelle versus associated with the cytosolic face of an organelle. Additionally, if an effector protein changes localization at different stages of infection, as has been demonstrated for SopB³⁶, these dynamic changes in localization can be visualized over time.

To test the ability of split-GFP to resolve organelle localization, we examined SlrP, which has been suggested to contain populations in both the cytosol and ER lumen³⁷. Transfected SlrP was found to localize to the cytosol, where it was suggested to function as an E3 ubiquitin ligase with thioredoxin as a binding partner²⁹. But, a later study identified the ER luminal chaperone ERdj3 as a potential binding partner, and suggested that transfected SlrP could localize to the ER³⁷. Motivated by the possibility of dual localization, we aimed to distinguish two distinct populations of SlrP versus a dynamic population that changes localization at different stages of the infection process. To assess these scenarios, we carried out long-term imaging of live cells infected with *Salmonella* expressing SlrP-GFP11, from 4–28 hours post infection. To exclusively visualize ER populations of SlrP, we used an ER lumen localized version of GFP1-10 (ER-GFP1-10)³⁸. Using ER-GFP1-10 together with the ER luminal protein disulfide isomerase tagged with GFP11³⁸ we verified that split-GFP localized to the ER gave rise to GFP_{comp} fluorescence (Fig. 5A). For SlrP, we consistently observed cytosolic complementation beginning at 7 hours post infection and continuing for the duration imaged (Fig. 5B), but didn't detect signal for SlrP-GFP_{comp} in the ER lumen at any time 4–28hrs post infection (Fig. 5C). The same localization was observed for plasmid-based expression of SlrP-GFP11 under the *steA* promoter as well as chromosomal expression of SlrP-1X-GFP11 and SlrP-3X-GFP11. Our results indicate that SlrP maintains a cytosolic C-terminus throughout 7–28 hrs post infection.

Visualization of effector proteins in primary macrophage cells using split-GFP

Salmonella target both epithelial cells and macrophages during infection of a host organism and these niches give rise to very different host-pathogen interfaces^{2,3,39,40}. The mode of *Salmonella* internalization, strategies used for intracellular survival, and fate of the infected host cell varies in epithelial cells versus macrophages and different pathogenicity islands, and their associated effector proteins have been implicated in setting up different niches in these cell types⁴⁰. But far less attention has been paid to possible differences in the roles

effector proteins may play between cell lines such as RAW264.7 cells and primary macrophages from different mouse models. Yet, the role of pathogenicity islands and the ability of *Salmonella* to replicate in RAW264.7 cells versus primary mouse macrophages versus human monocyte-derived macrophages in different activation states differs significantly^{12,41}. In this work, we set out to examine primary BMDMs from immunocompetent mice (SV129S6), as a model for systemic infection. SV129S6 mice contain a functional NRAMP1 metal transport protein and *Salmonella* can persist within macrophages of Nramp1^{+/+} mice for up to 1 year, establishing this system as a model for chronic infection⁴²⁻⁴⁴. In contrast, RAW264.7 cells are derived from immunocompromised NRAMP1^{-/-} mice and are commonly used as a model for acute infection. RAW264.7 cells have been shown to differ significantly from primary BMDMs in proteomics and phagosome maturation⁴⁵, as well as in their ability to promote intracellular replication¹².

In this study, we set out to develop approaches for applying the split-GFP effector labeling platform in primary BMDMs from immunocompetent mice to visualize effector proteins for the first time in living primary immune cells. BMDMs are challenging to transfect because they are highly differentiated, have decreased proliferation rates, and can be readily activated or undergo cell death upon exposure to foreign DNA⁴⁶. To overcome this limitation, we used Nucleofector™ Technology to express the GFP1-10^{47,48}. To further facilitate visualization, we incorporated a blue nuclear marker (NLS-mTagBFP2) downstream of the gene encoding GFP1-10, and separated by an internal ribosomal entry site (IRES). This construct facilitated identification of transfected cells since the GFP1-10 is non-fluorescent in the absence of complementation with GFP11. Nucleofection of GFP1-10-IRES-NLS-mTagBFP led to identification of transfected cells via visualization of blue nuclear fluorescence, and split-GFP complementation was confirmed via co-transfection of an ERK-GFP11 positive control (Fig. 6, Fig. S6).

We successfully visualized SlrP, SteA, PipB2, SseG and SseF in primary BMDMs (Fig. 6). SlrP-GFP_{comp} signal appeared diffuse and cytosolic, indicating that localization in BMDMs is consistent with that observed in HeLa cells. The localization of SteA, PipB2, SseG and SseF was consistent with localization to intracellular membranes and similar to the pattern of observed for LAMP-1 (Fig. S7), which is frequently used to mark the SCV. Intriguingly, we observed distinct differences in the localization of these effector proteins compared to RAW264.7 cells, suggesting a significantly different intracellular niche in the macrophage cell line versus primary macrophage from immunocompetent mice (Fig. 7). We previously found that SteA and PipB2 accumulated on the SCV and membrane tubules in both HeLa and RAW cells¹⁴. However, primary BMDMs often lack a compact SCV, and instead internalized bacteria are more commonly enclosed within a membrane-bound compartment but spread throughout the cell⁷ (Fig. S7), as was observed in infection of human monocyte-derived macrophages⁴¹. In the primary BMDMs used in this study, SteA, PipB2, SseG and SseF, generally colocalized with internalized bacteria, but consistent with the lack of a concentrated SCV, effector localization was more spread out on intracellular membranes. These results reveal different phenotypes, suggesting different niches, in different kinds of cells and demonstrate that the split-GFP effector protein labeling platform can be used in multiple cell types to study effector protein localization under different model infection conditions. These results suggest that effector proteins may play substantially different roles

in different niches. The tools developed here open up the possibility of comparing localization, dynamics and lifetime of effector proteins in different types of infected host cells to identify the different roles these effector proteins play in different infection models.

Summary

In order to invade and survive in multiple types of host cells, *Salmonella* and similar intracellular pathogens must adapt to diverse environments. The coordinated action of translocated effector proteins enables pathogens to modulate host cell signaling and transport processes to generate a protective niche, resulting in a highly dynamic interplay between the bacteria and the host cell. Unraveling the elements of this complex relationship and elucidating the roles of individual effector proteins in establishing *Salmonella*'s niche requires techniques that monitor bacteria together with translocated effector proteins within the different types of infected host cells, as different modes of infection and different intracellular environments may require different subsets of effector proteins. Live cell imaging holds enormous potential for defining the intracellular phenotypes of *Salmonella* infection at the single cell level, tracking the fate of intracellular bacteria and dynamic localization of effector proteins. The modular platform for split-GFP labeling developed in this work enables the amplification of fluorescent signals by tuning effector protein expression level or multimerizing the tag. Efficient detection of effector proteins is best achieved using plasmid-based expression with a strong promoter, like the *steA* promoter, or by using multiple repeats of GFP11. Additionally, expression of GFP1-10 along with a blue nuclear marker enables facile identification of GFP1-10 expressing cells and aids in verification of low complementation signals. Using these new tools, we visualized a number of different translocated effector proteins over many hours in living cells upon infection. Importantly, we demonstrate the ability of this tool to illuminate the intracellular niche in both epithelial cells and primary macrophages. There are some limitations of this new tool. In particular, robust visualization of lowly expressed effectors required overexpression which could lead to perturbation of localization or biochemical function. This could perhaps be addressed by engineering a split-FP with a higher inherent brightness.

METHODS

Information on bacterial strains and plasmids, culturing conditions, the bacterial expression assay, infections, and imaging are provided in Supporting Information.

Supplementary Material

Refer to Web version on PubMed Central for supplementary material.

Acknowledgments

We would like to acknowledge the following sources for financial support: NSF Career Award (MCB-0950411 to AEP), NIH T32 GM008732 (to MM), and Predoctoral Fellowship (F31 GM106644 to SEM).

ABBREVIATIONS

SCV *Salmonella* containing vacuole

| | |
|-------------|-------------------------------------|
| T3SS | Type 3 secretion system |
| BMDM | Bone marrow derived macrophage cell |

References

1. Cornelis GR. The type III secretion injectisome. *Nat Rev Microbiol.* 2006; 4:811–825. DOI: 10.1038/nrmicro1526 [PubMed: 17041629]
2. Ramos-Morales F. Impact of *Salmonella* enterica Type III Secretion System Effectors on the Eukaryotic Host Cell. *ISRN Cell Biol.* 2012; 2012doi: 10.5402/2012/787934
3. LaRock DL, Chaudhary A, Miller SI. *Salmonellae* interactions with host processes. *Nat Rev Microbiol.* 2015; 13:191–205. DOI: 10.1038/nrmicro3420 [PubMed: 25749450]
4. Galán JE. *Salmonella* interactions with host cells: type III secretion at work. *Annu Rev Cell Dev Biol.* 2001; 17:53–86. DOI: 10.1146/annurev.cellbio.17.1.53 [PubMed: 11687484]
5. Chakravorty D, Hansen-Wester I, Hensel M. *Salmonella* Pathogenicity Island 2 Mediates Protection of Intracellular *Salmonella* from Reactive Nitrogen Intermediates. *J Exp Med.* 2002; 195:1155–1166. DOI: 10.1084/jem.20011547 [PubMed: 11994420]
6. Figueira R, Holden DW. Functions of the *Salmonella* pathogenicity island 2 (SPI-2) type III secretion system effectors. *Microbiology.* 2012; 158:1147–1161. DOI: 10.1099/mic.0.058115-0 [PubMed: 22422755]
7. McQuate SE, Young AM, Silva-Herzog E, Bunker E, Hernandez M, de Chaumont F, Liu X, Detweiler CS, Palmer AE. Long-term live-cell imaging reveals new roles for *Salmonella* effector proteins SseG and SteA. *Cell Microbiol.* 2017; :e12641.doi: 10.1111/cmi.12641
8. Rajashekar R, Liebl D, Chikkaballi D, Liss V, Hensel M. Live Cell Imaging Reveals Novel Functions of *Salmonella enterica* SPI2-T3SS Effector Proteins in Remodeling of the Host Cell Endosomal System. *PLoS ONE.* 2014; 9:e115423.doi: 10.1371/journal.pone.0115423 [PubMed: 25522146]
9. Rosselin M, Virlogeux-Payant I, Roy C, Bottreau E, Sizaret PY, Mijouin L, Germon P, Caron E, Velge P, Wiedemann A. Rck of *Salmonella enterica*, subspecies enterica serovar Enteritidis, mediates Zipper-like internalization. *Cell Res.* 2010; 20:647–664. DOI: 10.1038/cr.2010.45 [PubMed: 20368731]
10. Velge P, Wiedemann A, Rosselin M, Abed N, Boumart Z, Chaussé AM, Grépinet O, Namdari F, Roche SM, Rossignol A, Virlogeux-Payant I. Multiplicity of *Salmonella* entry mechanisms, a new paradigm for *Salmonella* pathogenesis. *Microbiol Open.* 2012; 1:243–258. DOI: 10.1002/mbo3.28
11. Knodler LA, Vallance BA, Celli J, Winfree S, Hansen B, Montero M, Steele-Mortimer O. Dissemination of invasive *Salmonella* via bacterial-induced extrusion of mucosal epithelia. *Proc Natl Acad Sci.* 2010; 107:17733–17738. DOI: 10.1073/pnas.1006098107 [PubMed: 20876119]
12. Helaine S, Thompson JA, Watson KG, Liu M, Boyle C, Holden DW. Dynamics of intracellular bacterial replication at the single cell level. *Proc Natl Acad Sci.* 2010; 107:3746–3751. DOI: 10.1073/pnas.1000041107 [PubMed: 20133586]
13. Kuhle V, Jäckel D, Hensel M. Effector Proteins Encoded by *Salmonella* Pathogenicity Island 2 Interfere with the Microtubule Cytoskeleton after Translocation into Host Cells. *Traffic.* 2004; 5:356–370. DOI: 10.1111/j.1398-9219.2004.00179.x [PubMed: 15086785]
14. Van Engelenburg SB, Palmer AE. Imaging type-III secretion reveals dynamics and spatial segregation of *Salmonella* effectors. *Nat Meth.* 2010; 7:325–330. DOI: 10.1038/nmeth.1437
15. Galán JE, Lara-Tejero M, Marlovits TC, Wagner S. Bacterial Type III Secretion Systems: Specialized Nanomachines for Protein Delivery into Target Cells. *Annu Rev Microbiol.* 2014; 68:415–438. DOI: 10.1146/annurev-micro-092412-155725 [PubMed: 25002086]
16. Radics J, Königsmaier L, Marlovits TC. Structure of a pathogenic type 3 secretion system in action. *Nat Struct Mol Biol.* 2014; 21:82–87. DOI: 10.1038/nsmb.2722 [PubMed: 24317488]
17. Enninga J, Mounier J, Sansonetti P, Tran Van Nhieu G. Secretion of type III effectors into host cells in real time. *Nat Meth.* 2005; 2:959–965. DOI: 10.1038/nmeth804

18. Van Engelenburg SB, Palmer AE. Quantification of Real-Time *Salmonella* Effector Type III Secretion Kinetics Reveals Differential Secretion Rates for SopE2 and SptP. *Chem Biol.* 2008; 15:619–628. DOI: 10.1016/j.chembiol.2008.04.014 [PubMed: 18559272]
19. Charpentier X, Oswald E. Identification of the Secretion and Translocation Domain of the Enteropathogenic and Enterohemorrhagic *Escherichia coli* Effector Cif, Using TEM-1-Lactamase as a New Fluorescence-Based Reporter. *J Bacteriol.* 2004; 186:5486–5495. DOI: 10.1128/JB.186.16.5486-5495.2004 [PubMed: 15292151]
20. Mills E, Baruch K, Charpentier X, Kobi S, Rosenshine I. Real-Time Analysis of Effector Translocation by the Type III Secretion System of Enteropathogenic *Escherichia coli*. *Cell Host Microbe.* 2008; 3:104–113. DOI: 10.1016/j.chom.2007.11.007 [PubMed: 18312845]
21. Gawthorne JA, Audry L, McQuitty C, Dean P, Christie JM, Enninga J, Roe AJ. Visualizing the Translocation and Localization of Bacterial Type III Effector Proteins by Using a Genetically Encoded Reporter System. *Appl Environ Microbiol.* 2016; 82:2700–2708. DOI: 10.1128/AEM.03418-15 [PubMed: 26921426]
22. Knodler LA, Bestor A, Ma C, Hansen-Wester I, Hensel M, Vallance BA, Steele-Mortimer O. Cloning Vectors and Fluorescent Proteins Can Significantly Inhibit *Salmonella enterica* Virulence in Both Epithelial Cells and Macrophages: Implications for Bacterial Pathogenesis Studies. *Infect Immun.* 2005; 73:7027–7031. DOI: 10.1128/IAI.73.10.7027-7031.2005 [PubMed: 16177386]
23. Clark L, Martinez-Argudo I, Humphrey TJ, Jepson MA. GFP plasmid-induced defects in *Salmonella* invasion depend on plasmid architecture, not protein expression. *Microbiology.* 2009; 155:461–467. DOI: 10.1099/mic.0.025700-0 [PubMed: 19202094]
24. Xu X, Hensel M. Systematic Analysis of the SsrAB Virulon of *Salmonella enterica*. *Infect Immun.* 2009; 78:49–58. DOI: 10.1128/IAI.00931-09 [PubMed: 19858298]
25. Niemann GS, Brown RN, Mushamiri IT, Nguyen NT, Taiwo R, Stufkens A, Smith RD, Adkins JN, McDermott JE, Heffron F. RNA Type III Secretion Signals That Require Hfq. *J Bacteriol.* 2013; 195:2119–2125. DOI: 10.1128/JB.00024-13 [PubMed: 23396917]
26. Bajar BT, Lam AJ, Badiie RK, Oh YH, Chu J, Zhou XX, Kim N, Kim BB, Chung M, Yablonovitch AL, Cruz BF, Kulalert K, Tao JJ, Meyer T, Su XD, Lin MZ. Fluorescent indicators for simultaneous reporting of all four cell cycle phases. *Nat Meth.* 2016; doi: 10.1038/nmeth.4045
27. Kuhle V, Hensel M. SseF and SseG are translocated effectors of the type III secretion system of *Salmonella* pathogenicity island 2 that modulate aggregation of endosomal compartments. *Cell Microbiol.* 2002; 4:813–824. DOI: 10.1046/j.1462-5822.2002.00234.x [PubMed: 12464012]
28. Müller P, Chikkaballi D, Hensel M. Functional Dissection of SseF, a Membrane-Integral Effector Protein of Intracellular *Salmonella enterica*. *PLoS ONE.* 2012; 7:e35004. doi: 10.1371/journal.pone.0035004 [PubMed: 22529968]
29. Bernal-Bayard J, Ramos-Morales F. *Salmonella* type III secretion effector SlrP is an E3 ubiquitin ligase for mammalian thioredoxin. *J of Biol Chem.* 2009; 284:27587–27595. DOI: 10.1074/jbc.M109.010363 [PubMed: 19690162]
30. Layton AN, Brown PJ, Galyov EE. The *Salmonella* Translocated Effector SopA Is Targeted to the Mitochondria of Infected Cells. *Journal of Bacteriology.* 2005; 187:3565–3571. DOI: 10.1128/JB.187.10.3565-3571.2005 [PubMed: 15866946]
31. Kuhle V, Abrahams GL, Hensel M. Intracellular *Salmonella enterica* Redirect Exocytic Transport Processes in a *Salmonella* Pathogenicity Island 2-Dependent Manner. *Traffic.* 2006; 7:716–730. DOI: 10.1111/j.1600-0854.2006.00422.x [PubMed: 16637890]
32. Deiwick J, Salcedo SP, Boucrot E, Gilliland SM, Henry T, Petermann N, Waterman SR, Gorvel JP, Holden DW, Meresse S. The Translocated *Salmonella* Effector Proteins SseF and SseG Interact and Are Required To Establish an Intracellular Replication Niche. *Infect Immun.* 2006; 74:6965–6972. DOI: 10.1128/IAI.00648-06 [PubMed: 17015457]
33. Yu X-J, Liu M, Holden DW. *Salmonella* Effectors SseF and SseG Interact with Mammalian Protein ACBD3 (GCP60) To Anchor *Salmonella*-Containing Vacuoles at the Golgi Network. *mBio.* 2016; 7:e00474–16. DOI: 10.1128/mBio.00474-16 [PubMed: 27406559]
34. Abrahams GL, Müller P, Hensel M. Functional Dissection of SseF, a Type III Effector Protein Involved in Positioning the *Salmonella*-Containing Vacuole. *Traffic.* 2006; 7:950–965. DOI: 10.1111/j.1600-0854.2006.00454.x [PubMed: 16800847]

35. Guy RL, Gonias LA, Stein MA. Aggregation of host endosomes by *Salmonella* requires SPI2 translocation of SseFG and involves SpvR and the *fms*–*aroE* intragenic region. *Mol Microbiol.* 2000; 37:1417–1435. DOI: 10.1046/j.1365-2958.2000.02092.x [PubMed: 10998173]
36. Patel JC, Hueffer K, Lam TT, Galán JE. Diversification of a *Salmonella* Virulence Protein Function by Ubiquitin-Dependent Differential Localization. *Cell.* 2009; 137:283–294. DOI: 10.1016/j.cell.2009.01.056 [PubMed: 19379694]
37. Bernal-Bayard J, Cardenal-Munoz E, Ramos-Morales F. The *Salmonella* Type III Secretion Effector, *Salmonella* Leucine-rich Repeat Protein (SlrP), Targets the Human Chaperone ERdj3. *J Biol Chem.* 2010; 285:16360–16368. DOI: 10.1074/jbc.M110.100669 [PubMed: 20335166]
38. Hyun SI, Maruri-Avidal L, Moss B. Topology of Endoplasmic Reticulum-Associated Cellular and Viral Proteins Determined with Split-GFP. *Traffic.* 2015; 16:787–795. DOI: 10.1111/tra.12281 [PubMed: 25761760]
39. Malik-Kale P, Jolly CE, Lathrop S, Winfree S, Luterbach C, Steele-Mortimer O. *Salmonella* – At Home in the Host Cell. *Front Microbio.* 2011; 2:1–9. DOI: 10.3389/fmicb.2011.00125
40. Garai P, Gnanadhas DP, Chakravorty D. *Salmonella enterica* serovars Typhimurium and Typhi as model organisms: revealing paradigm of host-pathogen interactions. *virulence.* 2012; 3:377–388. DOI: 10.4161/viru.21087 [PubMed: 22722237]
41. Lathrop SK, Binder KA, Starr T, Cooper KG, Chong A, Carmody AB, Steele-Mortimer O. Replication of *Salmonella enterica* Serovar Typhimurium in Human Monocyte-Derived Macrophages. *Infect Immun.* 2015; 83:2661–2671. DOI: 10.1128/IAI.00033-15 [PubMed: 25895967]
42. Plant J, Glynn AA. Natural resistance to *Salmonella* infection, delayed hypersensitivity and Ir genes in different strains of mice. *Nature.* 1974; 248:345–347. DOI: 10.1038/248345a0 [PubMed: 4594698]
43. Monack DM, Bouley DM, Falkow S. *Salmonella typhimurium* persists within macrophages in the mesenteric lymph nodes of chronically infected *Nramp1*+/+ mice and can be reactivated by IFN γ neutralization. *J Exp Med.* 2004; 199:231–241. DOI: 10.1084/jem.20031319 [PubMed: 14734525]
44. Loomis WP, Johnson ML, Brasfield A, Blanc MP, Yi J, Miller SI, Cookson BT, Hajjar AM. Temporal and Anatomical Host Resistance to Chronic *Salmonella* Infection Is Quantitatively Dictated by *Nramp1* and Influenced by Host Genetic Background. *PLoS ONE.* 2014; 9:e111763.doi: 10.1371/journal.pone.0111763 [PubMed: 25350459]
45. Guo M, Härtlova A, Dill BD, Prescott AR, Gierliński M, Trost M. High-resolution quantitative proteome analysis reveals substantial differences between phagosomes of RAW 264.7 and bone marrow derived macrophages. *Proteomics.* 2015; 15:3169–3174. DOI: 10.1002/pmic.201400431 [PubMed: 25504905]
46. Zhang X, Edwards JP, Mosser DM. The expression of exogenous genes in macrophages: obstacles and opportunities. *Methods Mol Biol.* 2009; 531:123–143. DOI: 10.1007/978-1-59745-396-7_9 [PubMed: 19347315]
47. Maeß MB, Wittig B, Lorkowski S. Highly Efficient Transfection of Human THP-1 Macrophages by Nucleofection. *J Vis Exp.* 2014; 91doi: 10.3791/51960
48. Mullins CS, Wegner T, Klar E, Classen CF, Linnebacher M. Optimizing the process of nucleofection for professional antigen presenting cells. *BMC Res Notes.* 2015; 8:472.doi: 10.1186/s13104-015-1446-8 [PubMed: 26404473]

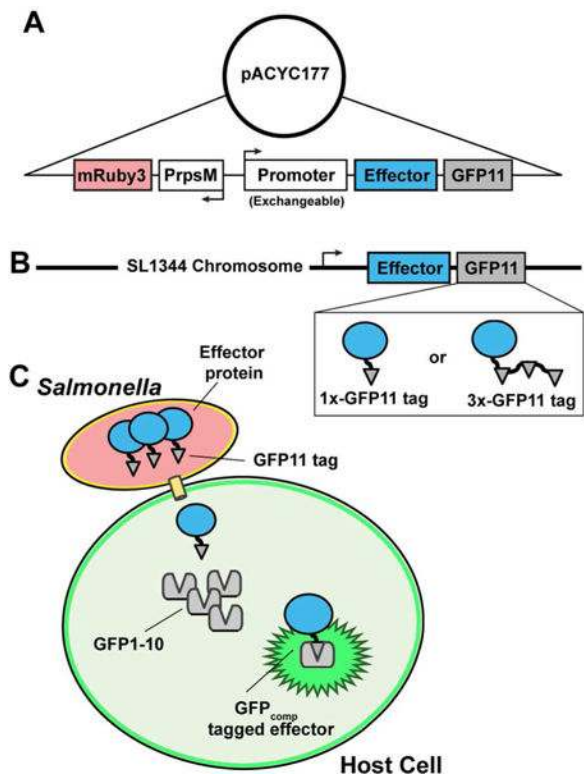


Figure 1. Platforms for labeling *Salmonella* effector proteins with split-GFP
 (A) The plasmid based effector protein-labeling platform with exchangeable promoters, effectors, and tags including a constitutive mRuby bacterial marker. (B) Chromosomally integrated effector-labeling using 1X-GFP11 or 3X-GFP11 tags. (C) Split-GFP effector protein-labeling to fluorescently tag and visualize effector proteins during infections of live host cells.

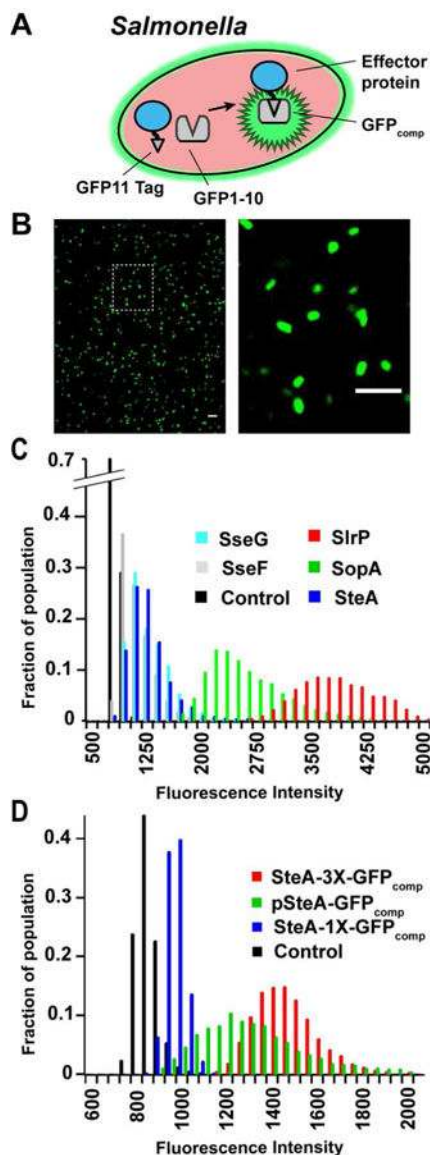


Figure 2. Bacterial expression assay to validate effector protein expression and split-GFP complementation efficiencies

(A) Chromosomally integrated or plasmid-based expression of GFP11-tagged effectors are expressed in bacteria alongside GFP1-10. The GFP_{comp} fluorescence signal is used to report on effector protein expression efficiency. (B) Representative image of GFP_{comp} fluorescence signal within bacteria used for automated ROI selection and analysis. Right image is a zoom in of box indicated by dashed line. (C) Representative effector protein expression and GFP-complementation levels for select bacterial strains using the plasmid based labeling platform. (D) The expression and GFP-complementation levels for SteA using chromosomal versus plasmid based labeling platforms. The control is a strain co-expressing GFP1-10 from pBAD and mRuby3 from the pACYC177 platform backbone in the absence of GFP11. Results represent the pooled total of 3 biological replicates, including 4 technical replicates per condition, $n_{\text{total}} \geq 1000$ bacteria (ROI) per condition.

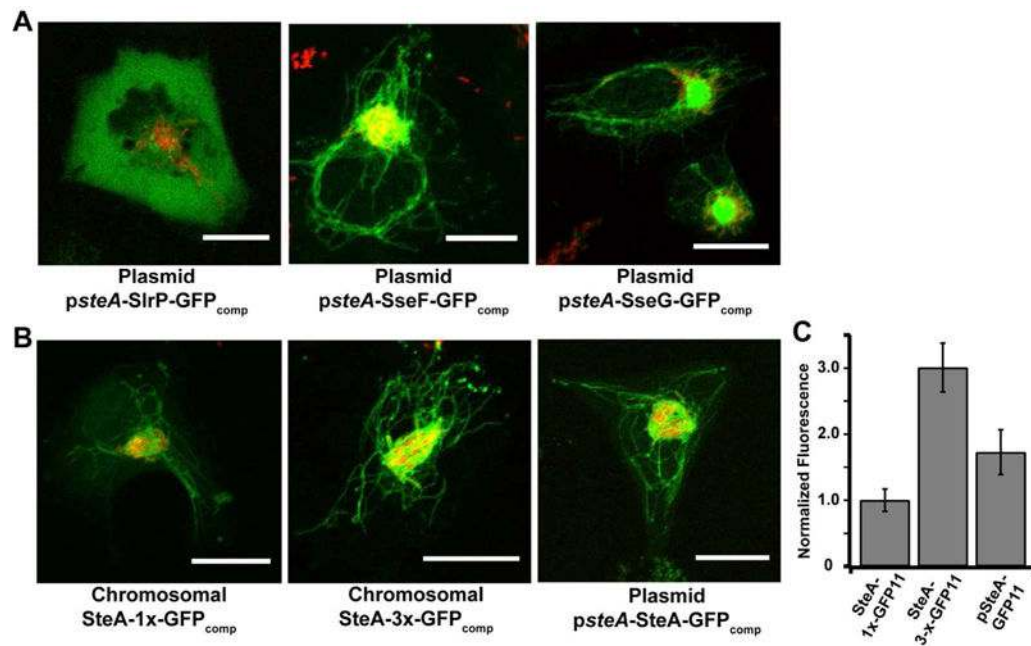


Figure 3. Visualizing translocated effector proteins inside live host cells

(A) The effector proteins SteA, SlrP, SseF, and SseG were expressed under the *steA* promoter for visualization in HeLa cells 16–20hrs post infection. Green is GFP_{comp} labeled effectors and red is *Salmonella* constitutively expressing mRuby3. Scale bars represent 20µm. (B) Plasmid and chromosomal based expression of SteA-GFP_{comp} or SteA-3xGFP_{comp} is visualized in HeLa cells 18hr post infection. GFP fluorescence was acquired for all images using identical settings and all images are scaled to the same intensity. Scale bars represent 20µm. (C) Average fluorescence intensities of SCV localized SteA-GFP_{comp} are compared for the plasmid based labeling platform for SteA-GFP11 versus chromosomal expression of SteA-1X-GFP11 and SteA-3X-GFP11. Fluorescence signal intensities are normalized to chromosomal SteA-1xGFP_{comp}. n = 20 per condition. Error bars are SD.

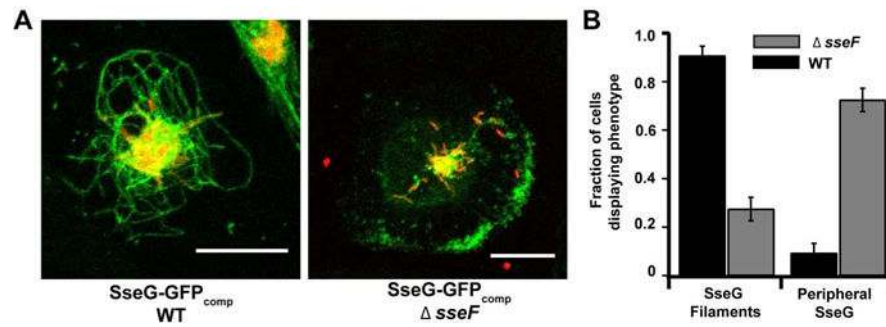


Figure 4. SseG gathers at the host cell periphery in the absence of SseF

(A) Representative images of infected HeLa cells at 14hrs post infection displaying localization of SseG-GFP_{comp} in the presence of SseF (WT, Left) and the absence of SseF ($\Delta sseF$, Right). (B) Average fraction of infected cells that display SseG-GFP_{comp} uniformly distributed across filaments compared to cells that contain SseG-GFP_{comp} aggregates at the host cell periphery. ntotal = 65 cells ($\Delta sseF$), 73 cells (WT). Error bars are SD across 3 separate infection experiments.

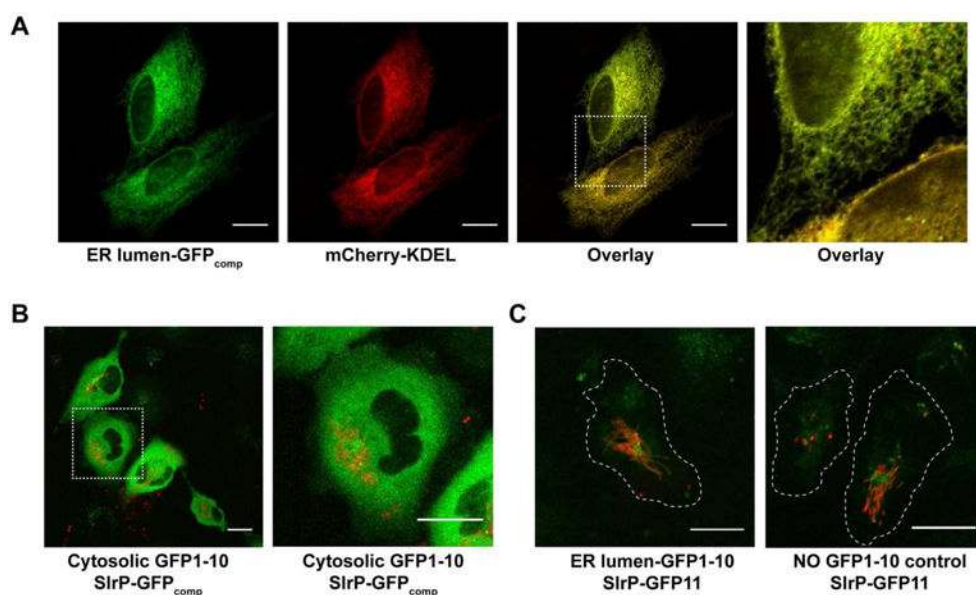


Figure 5. Defining subcellular localization of SlrP during live cell infections

(A) Split-GFP components were localized to the ER lumen for complementation and fluorescence signal verification. (B,C) Host cells expressing cytosolic GFP1-10 (B) or ER localized GFP1-10 (C) were infected with *Salmonella* expressing SlrP-GFP11. (B) Representative infected cells transiently expressing cytosolic GFP1-10. Second panel shows a zoomed in perspective. (C) Representative infected cells with and without transient expression of ER localized GFP1-10. GFP fluorescence was acquired for all images using identical settings and all images are scaled to the same intensity. Scale bars represent 20 μ m.

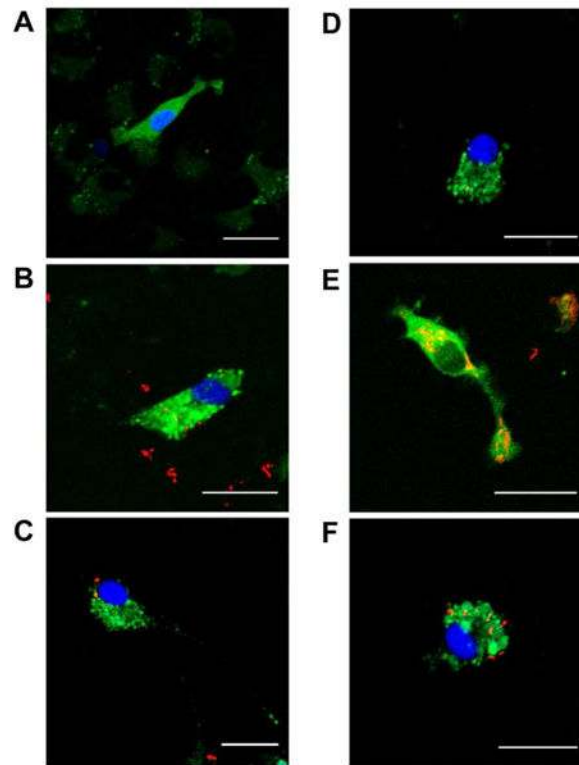


Figure 6. Fluorescence images demonstrating split-GFP fluorescence complementation in BMDMs nucleofected with GFP1-10-IRES-NLS-mTagBFP2

Fluorescence overlay (blue NLS)mTagBFP2, green GFP_{comp}, red mRuby3 in *Salmonella* images of bone marrow derived macrophages expressing GFP1-10-IRES-NLS-mTagBFP2. (A) Cells were co-transfected with ERK-GFP11 as a positive control. (B–F) Representative cells nucleofected with GFP1-10-IRES-NLS-mTagBFP2 and infected with *Salmonella* strains expressing mRuby3 and the specified effector tagged with GFP-11. Representative images collected from 12–14 hours post infection are shown for (B) SseF-GFP_{comp}, (C) PipB2-GFP_{comp}, (D) SteA-GFP_{comp}, (E) SlrP-GFP_{comp}, and (F) SseG-GFP_{comp}.

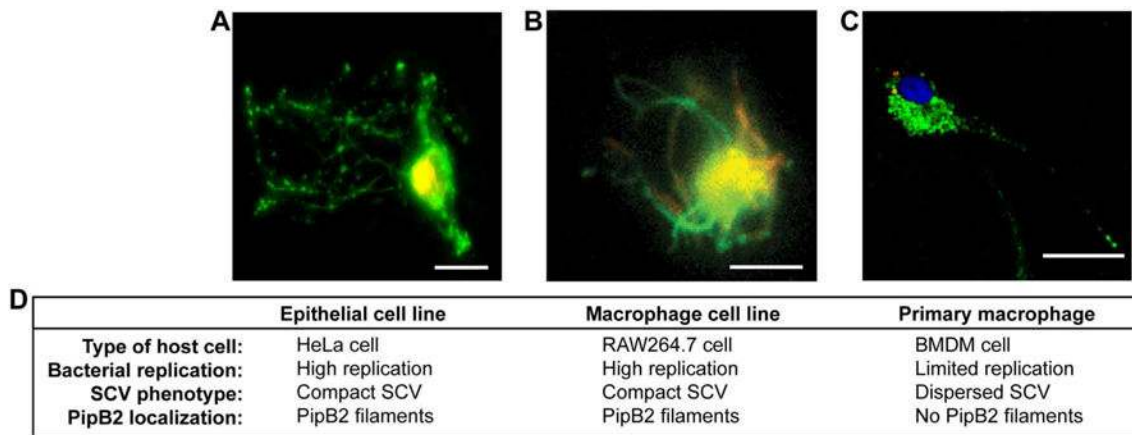


Figure 7. *Salmonella* infection of different host cell types results in different intracellular niches

Representative images of different types of host cells infected with *Salmonella* (red) displaying PipB2-GFP_{comp} fluorescence (green) are compared. An infected HeLa cell (A), RAW264.7 cell (image modified from Van Engelenburg and Palmer 2010)¹⁶ (B), and a primary BMDM cell (C) are shown. The observed phenotypes for bacterial replication, SCV appearance and PipB2 localization are detailed (D) for the different infected cell types. Scale bars are 20µm.

Table 1

Comparison of bacterial expression assay and split-GFP complementation in infected host cells

| PLASMID EXPRESSION UNDER <i>steA</i> PROMOTER | | | |
|--|-------------------------|-------------------|-----------------------------------|
| Promoter | Effector Protein | Expression | Visualization in Host Cell |
| <i>steA</i> | SteA | ++ | Y |
| | SlrP | +++++ | Y |
| | SseF | + | Y |
| | SseG | ++ | Y |
| | SopA | ++++ | <i>N</i> |
| PLASMID EXPRESSION UNDER ENDOGENOUS PROMOTERS | | | |
| Promoter | Effector Protein | Expression | Visualization in Host Cell |
| <i>slrP</i> | SlrP | + | <i>N</i> |
| <i>sseA</i> | SseF | + | Y |
| <i>sseA</i> | SseG | - | <i>N</i> |
| <i>sopA</i> | SopA | +++ | <i>N</i> |
| CHROMOSOMAL EXPRESSION | | | |
| Effector Protein | Tag | Expression | Visualization in Host Cell |
| SteA | 1x-GFP11 | + | Y |
| | 3x-GFP11 | ++++ | Y |
| SlrP | 1x-GFP11 | - | <i>N</i> |
| | 3x-GFP11 | + | <i>N</i> |
| SseF | 1x-GFP11 | - | <i>N</i> |
| | 3x-GFP11 | - | <i>N</i> |
| SseG | 1x-GFP11 | - | <i>N</i> |
| | 3x-GFP11 | - | <i>N</i> |

The bacterial expression assay from Figure 2D was quantified as follows: - represents no detection of fluorescence signal above the negative control, + is the major peak of fluorescence signal within a population is within 1 standard deviation of the negative control, +++ is within 3 standard deviations of the negative control and so on. Visualization within infected host cells was assessed for each condition between 4–24 hrs post infection, where Y indicates that effector-GFP_{comp} signal was detectable above background, N indicates no detectable GFP_{comp} signal.